



Particle-Size-Dependent Filtration Efficiency, Breathability, and Flow Resistance of Face Coverings and Common Household Fabrics Used for Face Masks During the COVID-19 Pandemic

Olukayode James Ayodeji¹ · Terrell A. Hilliard¹ · Seshadri Ramkumar¹ 

Received: 6 September 2021 / Revised: 24 December 2021 / Accepted: 27 December 2021 / Published online: 10 January 2022
© University of Tehran 2022

Abstract

During the COVID-19 pandemic, the increase in demand for protective equipment caused a global shortage and homemade barrier face coverings were recommended as alternatives. However, filtration performances of homemade face coverings have not been fully evaluated. Test methods in the ASTM standard (F3502-21) were used to evaluate filtration efficiencies (FE) and breathability (pressure drop, Δp) of face coverings and home fabric materials commonly used during the pandemic. Submicron particulates FE was measured by particle transmission through face covering samples using a Condensation Particle Counter equipped with differential mobility analyzer and electronic manometer. Flow resistance of 0.1 μm -diameter fluorescent nanoparticles in droplets was determined by measuring fluorescence intensity of residual collected at the reverse side of samples. The size-dependent FE (3–94%) and Δp (0.8–72 mmH_2O) varied considerably among fabrics. Of the 16 mask types, 31.25% and 81.25% met the minimum FE and breathability standards in the ASTM F3502-21, respectively. Overall performance (qF) was highest for velcro masks (max qF = 3.36, min qF = 2.80) and lowest for Dutch wax print fabrics (max qF = 0.12, min qF = 0.03). Most of the samples resisted the flow of 0.1 μm -diameter nanoparticles in droplets. Low flow resistance was observed in bandana, neck gaiter, t-shirt I, tank top and bedspread fabrics. GSM and fabric finishing seems to affect performance. Low performances can be improved by selecting optimum-performance fabrics in the design and manufacture of barrier face coverings.

Article Highlights

- Face coverings protect both the wearer and others against severe acute respiratory diseases.
- Shortage of personal protective equipment resulted in the use of homemade face coverings.
- Standardized test revealed filtration efficiency and breathability that varied among fabric samples.
- Tested materials and multiple layers are recommended for use in alternative face coverings production.

Keywords Filtration · Pressure differentiation · Face covering · COVID-19 · Flow resistance

Introduction

The outbreak of the COVID-19 pandemic has significantly impacted the social interactions, economy, culture, and health of billions of people around the globe (Gopalan and

Misra 2020; Mofijur et al. 2021). During the outbreak, widespread lockdowns, physical and social distancing (Drewnick et al. 2021; Marroquin et al. 2020), travel restrictions (Beck and Hensher 2020), and wearing of face coverings (Ayodeji and Ramkumar 2021; Zhang et al. 2020) were the major mitigation measures to protect public health. The wearing of face coverings followed recommendations from the World Health Organization and the United States Centers for Disease Control (CDC) that barrier face coverings protect both the wearer and others from infection through exposure to droplets and aerosols carrying infectious virus (CDC 2020a;

✉ Seshadri Ramkumar
s.ramkumar@ttu.edu

¹ Department of Environmental Toxicology, The Institute of Environmental and Human Health, Texas Tech University, Lubbock, TX 79416, USA

b; WHO 2020a, b). According to Johnson et al. (2011), humans emit respiratory droplets with three distinct size distribution modes of 1.6, 2.5 and 145 μm when they speak and 1.6, 1.7 and 123 μm (median diameters) when they cough.

The use of face coverings has become prevalent globally in response to the COVID-19 pandemic, because SARS-CoV-2 can be transmitted via respiratory droplets (National Academies of Sciences, Engineering, and Medicine 2020; WHO 2020b). The use of barrier face coverings is also an anticipated public response in the face of future pandemics related to severe acute respiratory syndromes (Konda et al. 2020) just as it was used in the past (Syed et al. 2003). The resulting increase in demand for protective face masks during the COVID-19 pandemic has caused a severe global shortage. Because aerosols and droplets can be removed by the fibers of fabrics through a series of filtration mechanisms, homemade or purchased cloth face coverings were, therefore, recommended as alternatives in situations, where face masks are not available (CDC 2020b; Kwong et al. 2021).

Through the mechanisms of inertia impaction, gravitational sedimentation, interception, diffusion, and electrostatic attraction, materials can remove airborne particles by filtration (Hinds 1999; Vincent 2007). Larger sized aerosols (1–10 μm) are more effectively removed by impaction and interception, smaller sized particles (< 0.1 μm) are more effectively removed via diffusion by Brownian motion (Friedlander 2000), and gravitational forces are the major influence on the much larger droplets (Konda et al. 2020). Nanometer-sized aerosols are predominantly removed by electrostatic interaction (Konda et al. 2020). The major components of facemasks are the ability of their materials to achieve a high filtration efficiency (FE) of particulates and droplet flow resistance, while sufficient breathability and comfort is sustained (Hao et al. 2020; Kähler and Hain 2020; Kwong et al. 2021; Zhao et al. 2020). The ease of breathing through a barrier face covering is typically measured by the pressure differential (or pressure drop, Δp) between the two sides of the face covering as air flows through it (Kwong et al. 2021) especially when measured at a rate similar to that of a normal breathing range of 3.3 – 27.2 cm/s (Jones and Rempel 2021). Higher Δp is an indication that it is harder to breathe through a fabric or face covering, while lower Δp indicates that the mask is more breathable.

While non-medical and homemade barrier face coverings have been widely used during the COVID-19 pandemic (Aydin et al. 2020; Hao et al. 2021; Joo et al. 2021), their filtration performances have not been fully evaluated and documented (CDC 2020b; Hao et al. 2020; Liu and Zhao 2021). The ability of a barrier face covering to protect the wearers and others is dependent on both the mask materials and design (Kwong et al. 2021). As reviewed by Kwong et al. (2021), a number of recently published studies have

evaluated the FE and breathability of various face coverings and homemade face covering fabrics. It was highlighted that the major limitations of these studies include inadequate description of fabric materials evaluated in the studies, inability to replicate experiments, the use of unstandardized methodologies, and wide variability in key parameters, such as type of particles, volumetric flow (face velocity), and area of material under test. These have created uncertainties in the choice of materials for homemade barrier face coverings (Kwong et al. 2021). Therefore, the collection of empirical data sets on the performance of non-medical face covering materials is urgently needed to guide mitigation strategies in situations when medical supplies are limited or unavailable (Hao et al. 2020).

In addition, different filtration rating systems have been developed to evaluate filtration performances for different particle size ranges. These systems include microparticle performance rating (MPR, designed by 3 M), minimum efficiency reporting value (MERV, designed by the American Society of Heating, Refrigerating and Air-Conditioning Engineers), and filter performance rating (FPR, by the Home Depot). These ratings are not designed for homemade face-masks (Hao et al. 2020). In addition, specialized equipment recommended by the National Institute for Occupational Safety and Health (NIOSH) for certification and FE testing may not be affordable to the manufacturers of homemade face coverings (Kwong et al. 2021). In February 2021, American Society for Testing and Materials (ASTM) standard (F3502-21) was approved and primarily introduced in response to the COVID-19 pandemic. It was intended to help ensure that barrier face coverings meet the requirements of source control of expelled droplets and aerosols by individual wearers. It is also to ensure a degree of particulate filtration to minimize the amount of inhaled particulate matter (ASTM 2021). The standard specified area of sample to be tested, face velocity, flow rate, FE performance range, breathability range, test temperature, and relative humidity, among others.

This represents the first study that utilizes standardized methods to evaluate home fabrics as alternative materials for barrier face coverings. The objectives of the current study are (1) to characterize and evaluate the performances (FE, Δp , and qF) of commonly used barrier face coverings and household fabrics for face coverings and (2) to provide data sets that guide the selection of materials for the production of homemade barrier face coverings. These objectives were accomplished by utilizing the test methods in the recent ASTM Standard (F3502-21: Specification for Barrier Face Coverings).

Materials and Methods

Reagents, Microspheres, and Barrier Face Coverings

Reagents used are provided in supplementary information. Six commonly used barrier face covering were purchased from open markets. They were fashion face masks, bandana, velcro mask (with inner activated carbon filters), cotton face covering, neck gaiter and surgical masks. Ten samples of common house fabrics were sourced from households, and they include denim/jean, polo-style shirt, t-shirt I and II (different material compositions), collared shirt, tank top, towel, bedspread, pillowcase, and Dutch wax print fabric. Both N95 and R95 masks have FE of at least 95% but R95 masks (3 M-8247) were used as reference in the current study because of their additional characteristic of oil resistance (CDC 1996). Samples images are provided in Supplementary Fig. 1.

Fabric Characterization

Samples were numbered 1–16. To quantify fabric density (grams per square meter—GSM), rectangular or square samples were cut from each sample and weighted using a precision laboratory weighing scale. Area was calculated from the dimension ($L \times B$, m^2). GSM was then computed for each sample. Material composition of fabric samples (cotton, polyester, spandex, polypropylene contents) were recorded from fabric manufacturers' labels. Samples were visually inspected to determine construction style (woven, knitted or piled). For the already-made face coverings that were purchased, number of plies was determined by counting observed layers after cutting.

Particulates Generation and Challenge

Submicron particulate sizes included in the study were 0.03, 0.04, 0.05, 0.06, 0.08, 0.10, 0.15, 0.20, 0.25, 0.30, 0.35, and 0.40 μm -diameter. Particle size selection was to mimic the size range of SARS-CoV-2 virus (0.07–0.10 μm -diameter, Aydin et al. 2020). Selection was also based on previously reported tested size ranges, size distribution of SARS-CoV-2-laden aerosols (Konda et al. 2020; Liu et al. 2020), and guide for filter certification (CDC 1996; Kwong et al. 2021). Test methods in the ASTM Standard (F3502-21) were used to test particle-size dependent FE and breathability with only two exceptions. Samples are required to be pre-conditioned at $85 \pm 5\%$ relative humidity and 38 ± 2.5 °C for 25 ± 1 h. Omitting these two requirements is supported for products not designed to meet NIOSH certification as previously discussed by Cho et al. (2011). Area under test for each sample

was 50 cm^2 with a constant face velocity of 10 ± 0.5 cm/s and flow rate of 32 ± 0.5 l/min as specified in the ASTM Standard.

Previously described experimental methods (Cho et al. 2011; Drewnick et al. 2021; Hao et al. 2021) were slightly modified. In the present study, Dioctyl Phthalate (DOP) oil was used to generate the submicron particles (Cho et al. 2011). Briefly, FE of samples was determined by measuring particle transmission through each sample with a TSI Certitest® Automated Filter Tester (Model 3160) using two Condensation Particle Counters (CPC Model 3771) equipped with a differential mobility analyzer (DMA, model 308,100) and an aerosol neutralizer (model 3077) with a Krypton—85 source. DOP oil was used to generate aerosol particles ($d = 0.03$ – 0.4 μm) using DOP atomizers, electrostatic classifier (Model 3080), and a silica gel desiccant as air supply dryer. Air flow was controlled by a vacuum pump and an adjustable valve and measured by a mass flowmeter (l/min) (Model 4043).

The DMA was used to generate poly-disperse aerosols of the desired diameter which were then passed through another neutralizer. After dilution (Aerosol Diluter, Model 3302) with particle-free air and mixing, the generated aerosol particulates pass through the sample in a sample holder plate (7.98 cm —diameter, 50.01 cm^2 —area). The first CPC measured upstream aerosol concentration, while the second measured the concentration downstream of the sample holder. As part of quality assurance/quality control (QA/QC) protocol, a TSI Green Line Paper (HE—1071) of a known particle penetration and efficiency at a specific pressure was tested in every 3 sample runs ($n = 6$) to monitor analytical accuracy. A Schematic presentation of the CPC setup is shown in Supplementary Fig. 2. An electronic manometer (Model 220, all TSI Inc.) measured Δp across the two surfaces of the samples. Pressure measurement accuracy was 0.15% of reading.

Filtration Efficiency, Pressure Differentiation and Performance

As previously described by Li et al. (2018) and Hao et al. (2021), size-resolved number-based FE (ηN) was computed using the following equation:

$$\eta N = 1 - N_o/N_i, \quad (1)$$

where N_o and N_i are the measured downstream and upstream concentrations of aerosol at the filter holder. FE for each sample was computed and presented as percentages (%) and standard deviation (\pm SD) or standard error (\pm SE). GSM was used in analyses as an indicator for FE and Δp , because it correlates with material thickness (Hao et al. 2021). Spearman rank correlation (r_s) analysis was performed to evaluate

the relationship between GSM and $FE/\Delta p$. The overall performance of a barrier face covering is a function of its FE and breathability (Δp). A good barrier face cover should have a combined higher FE and lower Δp . Therefore, the present study used Eq. (2) (Drewnick et al. 2021; Hao et al. 2021) to evaluate the overall performance (qF) of each face covering material:

$$qF = \ln(1/P)/\Delta p, \quad (2)$$

where P is penetration efficiency ($= 1 - FE$) and Δp is the pressure differential (in kPa) across the samples. Higher qF values indicate an overall higher filtration performance. Relative performance (Rp) of samples was computed by finding the ratio of qF for samples and the qF for R95 using the following equation:

$$Rp = qF(s)/qF(R95). \quad (3)$$

Latex Beads Challenge and Droplet Resistance

Experimental setup previously described by Aydin et al. (2020) was slightly modified to evaluate droplet resistance of samples. Detailed description is provided in supplementary information. Briefly, a solution containing red fluorescent nanoparticles in deionized water was prepared. To challenge the barrier face covering samples, a mist sprayer was used to generate and discharge 200 ± 20 μL droplets of the challenge solution at 0.7 cm distance from the samples to mimic the closeness of nostril/mouth of wearer to the inner surface of face coverings. A petri dish was covered with a sample cut-out and attached to the rim of the dish using a rubber band. After discharging the droplets and impaction, nanobeads that penetrated the sample were collected in the petri dish and recovered in 100 μL water. Flow was determined by measuring fluorescence of beads in the 100 μL mix. As part of QA/QC protocol, 100 μL of the challenge solution was serially diluted to determine dilution factor. In addition, percentage recoveries of 2.5, 5.0 and 20 μL challenge solution were computed using Eq. (4). Percentage flow of fluorescent nanoparticles was determined using Eq. (5).

Percentage recovery was computed using Eq. (4). Percentage flow of fluorescent nanoparticles was determined using Eq. (5):

$$\text{Percentage recovery (\%)} = (IA/IB) \times 100, \quad (4)$$

where IA and IB are fluorescent intensities in Batch A and B, respectively:

$$\text{Flow (\%)} = (I_{\text{sample}}/I_{\text{solution}}) \times DF \times 100, \quad (5)$$

where I_{sample} is fluorescence intensity in 100 μL from the recovered 200 μL incident challenge solution, I_{solution} is

fluorescent intensity in 100 μL of the challenge solution, and DF is dilution factor.

Statistical Analyses

Each mask types and fabrics were replicated five times ($n = 5$) for all the experiments. Statistical analyses were performed with Statgraphs (v. 19.2.01) and IBM SPSS (v. 27). Tables and charts (with error bars) were constructed using Microsoft Excel (2010). Results were presented as arithmetic mean (\pm SD or \pm SE).

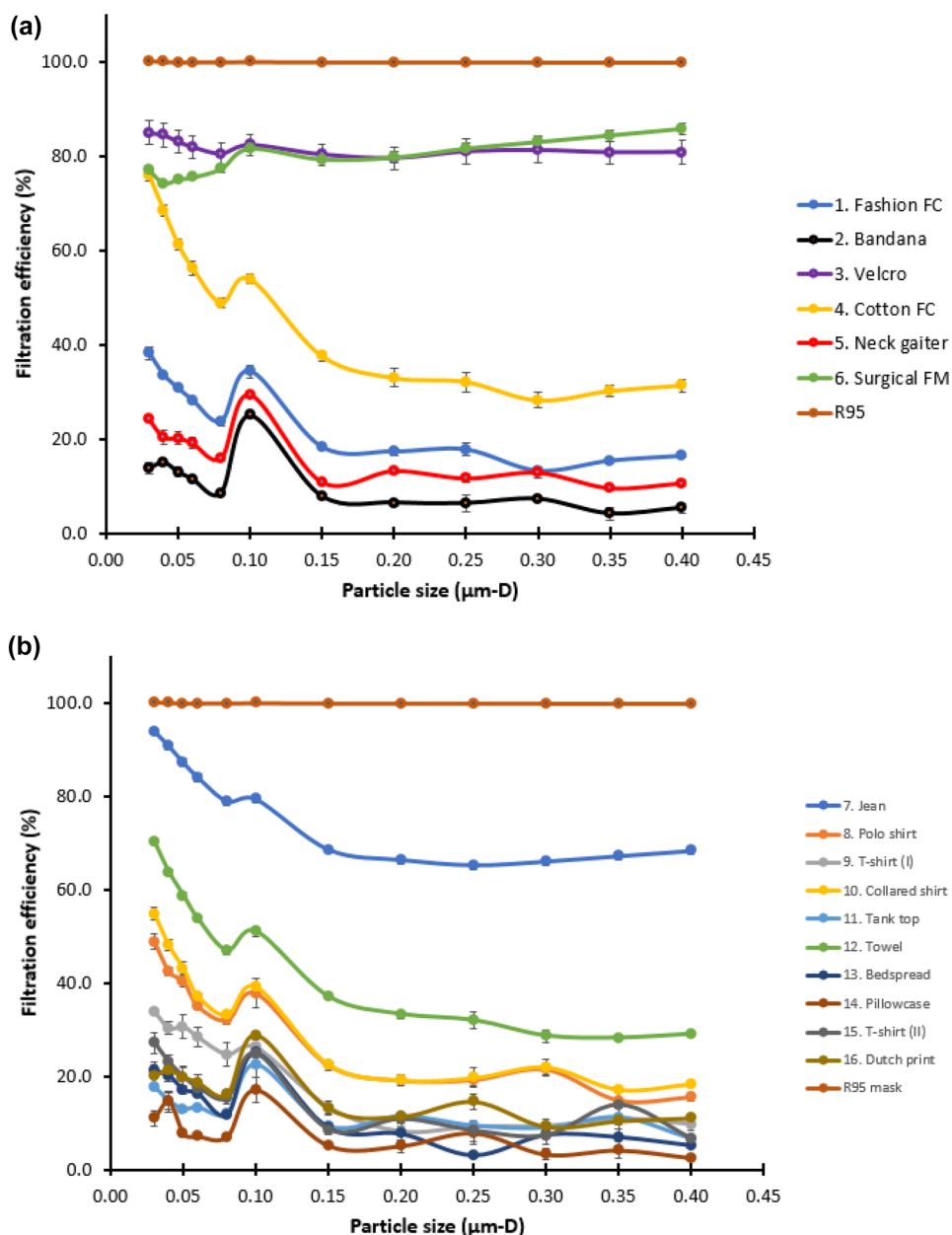
Results and Discussion

Size-Dependent Filtration Efficiency

A detailed description of the samples included in the present study, including fabric characterization and grams per square meter (GSM- g/m^2), is provided in Supplementary Table (S. Table) 1a and b. The size-dependent FE of each barrier face covering, and double-layer home fabric material are presented in S. Table 2. The use of barrier face coverings in future SARS-related pandemics remains a possibility (Konda et al. 2020), and the size of the causative viruses varies widely (Abdelrahman et al. 2020). In addition, research results have indicated that different material samples have different particle FE as a function of particle diameter (Joo et al. 2021) as noticeable in the current study (Fig. 1a, b). For most samples, FE was higher for particle size 0.03–0.08 μm . Particle size 0.1 μm has a distinctively higher FE before a slight reduction with increasing particle size. Particle size 0.3 μm -D is within the most penetrating particle size (MPPS, low FE) range.

For particle size 0.06 μm -d, the lowest FE was recorded for pillowcase fabric (7.14%), bandana face covering (11.48%), and tank top fabric (13.30%), while denim (84.00%), velcro mask (81.88%), and surgical mask (75.46%) were the highest. For particle size 0.1 μm -d, pillowcase (17.05%), tank top (22.56%), and t-shirt II (24.84%) have the lowest FE, while velcro mask (82.34%), surgical mask (81.53%), and denim fabric (79.36%) have the highest. Except for denim, polo-style fabric (only at 0.03 μm -D), collared shirt (only at 0.03–0.04 μm -D), and towel (only at 0.03–0.10 μm -D), all home fabric samples showed particle FE lower than 45% in the entire particle size range. It is noteworthy that bandana and neck gaiter showed FE lower than 30% in the entire size range (S. Table 2). FE across the entire size range were compared with ASTM (F3502-21) values of <20% for lower performance and >50% for higher performance barrier face coverings. R95 (3 M) masks were included as reference for performance comparison. Results are presented in Fig. 2a–e. Of all the ready-made barrier

Fig. 1 Size-dependent FE of barrier face coverings and home fabric samples. **a** Represents FE for already-made commonly used masks, and **b** represents FE for common household fabrics



face covering samples included in the present study, 68.75% have at least one size-dependent FE that is less than 20%, while 81.25% have at least one FE that is less than 50%. All home fabric samples have FE below 50%, except collared shirt (only at 0.03 µm-D) and denim (all sizes). Similar results were documented by Drewnick et al. (2021) for 0.03–0.25 µm diameter particles at both lower (5.3 cm/s) and higher (12.9 cm/s) face velocities. Double-layer neck gaiter and bandana have FE below 30% for all particle sizes (S. Table 2).

In the present study, statistically significant ($p < 0.05$) positive correlation was observed between GSM and FE (Table 1), that is, the higher the density of the tested samples,

the higher is the FE. The observed relationship is also size-dependent, because FE progressively decrease with increasing particulate diameter (S. Table 2). The relationship was supported by research outcome reported by Joo et al. (2021) that observed higher filtration performance for material samples with higher density. For home fabrics, towel (430.89 g/m²), denim (407.74 g/m²), and polo-style shirt (210.69 g/m²) have higher density with size-dependent FE range of 28.20–70.17%, 65.23–93.88% and 14.82–48.84%, respectively. On the other hand, Dutch wax print fabric (94.57 g/m²), t-shirt I (116.66 g/m²), and bedspread (118.07 g/m²) are fabric samples with lower density and respective lower FE range of 9.26–28.79%, 8.09–33.84%, and 3.11–25.00%.

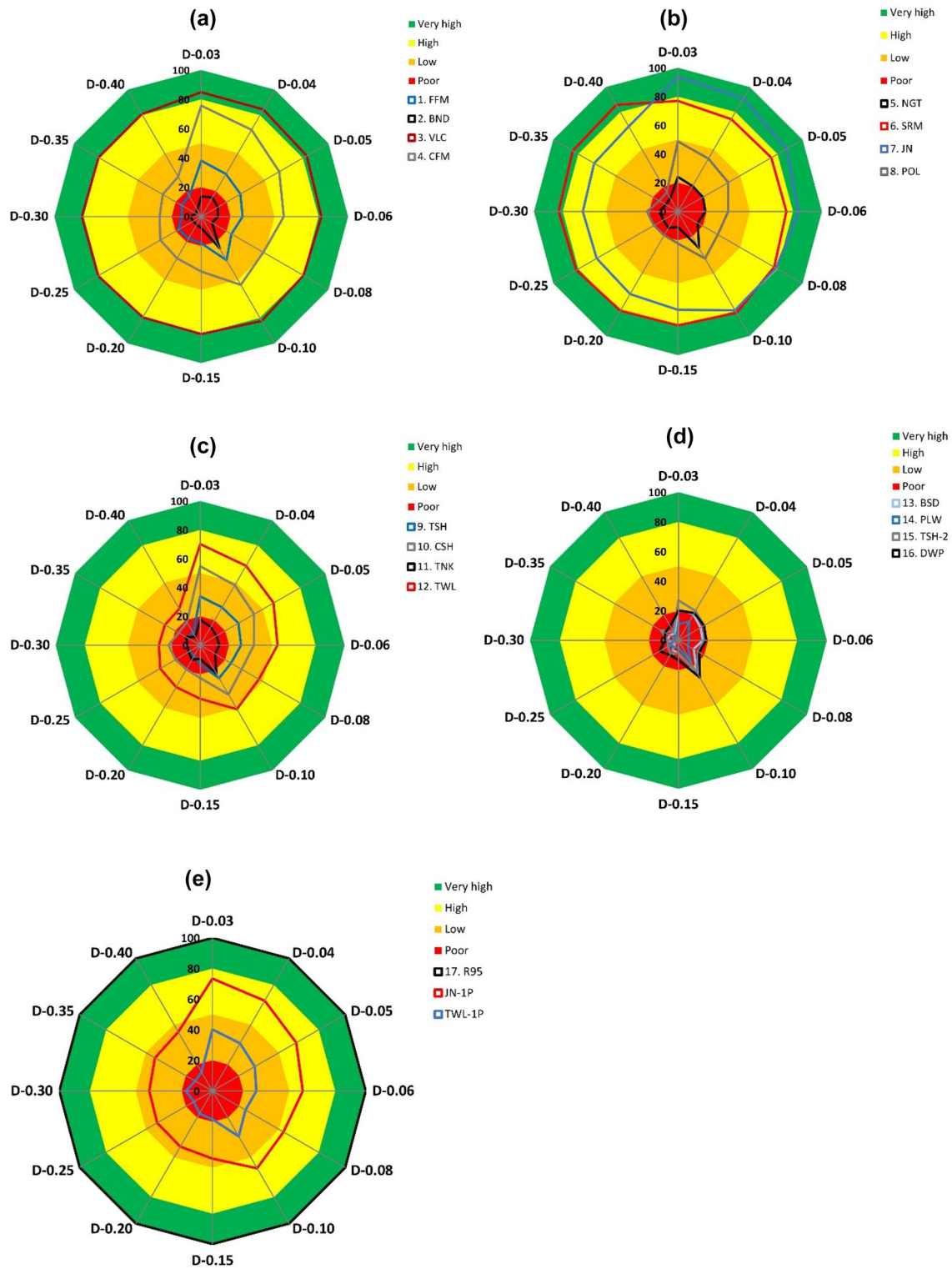


Fig. 2 Radar plots showing average FE of face coverings ($n=5$) compared with the ASTM standard (F3502-21) across the entire size range. The green area represents the FE category for very high-performance ($\geq 80\%$) masks, the yellow and orange areas represent mid-performance (20–80%) masks, while the red area represents masks with low performance ($\leq 20\%$). Keys: *D* diameter (μm), *FFM* fashion

mask, *BND* bandana, *VLC* velcro mask, *CFM* cotton mask, *NGT* neck gaiter, *SRM* surgical mask, *JN* jean/denim fabric, *POL* polo-style shirt fabric, *TSH* t-shirt I, *CSH* collared shirt, *TNK* tank top, *TWL* towel, *BSD* bedspread, *PLW* pillowcase, *TSH-2* t-shirt II, *DWP* Dutch wax print, *R95* 3 M R95 mask, *JNP-1P* single layer jean/denim fabric, *TWL-1P* single layer towel

Table 1 Correlation between FE/ Δp and GSM

Size (μm)	FE		Δp	
	<i>p</i> value	<i>r_s</i>	<i>p</i> value	<i>r_s</i>
0.03	0.017*	0.596	0.121	0.342
0.040	0.024*	0.564	0.134	0.375
0.050	0.021*	0.578	0.134	0.375
0.060	0.024*	0.564	0.179	0.336
0.080	0.027*	0.554	0.179	0.336
0.100	0.027*	0.554	0.179	0.336
0.150	0.030*	0.542	0.179	0.336
0.200	0.020*	0.581	0.179	0.336
0.250	0.027*	0.554	0.179	0.336
0.300	0.027*	0.552	0.179	0.336
0.350	0.025*	0.559	0.179	0.336
0.400	0.032*	0.537	0.179	0.336

*Significant at $p < 0.05$

Fiber contents or knitted/woven characterization appeared not to impact FE. Although the increase in FE with increasing GSM can be translated to increasing the number of layers to achieve higher FE performance, the impact on breathability deserves attention.

Breathability of Samples

Pressure differentiation values and patterns were very similar within face covering samples regardless of particulate size. Only minor variations were observed (S. Table 3). Therefore, only 0.03, 0.06, and 0.1 ($\mu\text{m-D}$) were selected for face coverings' breathability comparisons among samples (Fig. 3). Other size-sample comparisons are given in S. Fig. 3. The need for alternative materials for use in barrier face coverings is unprecedented. Acceptable material must be effective in slowing the spread of respiratory diseases by adequately filtering respiratory droplets and aerosols that might contain causative viruses yet providing sufficient breathability. In the present study, breathability is observed to decrease (increasing Δp) with increasing FE. An optimal high-performance face covering must have high FE, high breathability (low Δp), and be washable without performance compromise (Bagheri et al. 2021).

The highest breathability was observed for tank top (0.781–0.801 mmH_2O), t-shirt I (1.039–1.055 mmH_2O), and bandana (1.447–1.464 mmH_2O), while the lowest was noticed in denim (71.425–71.604 mmH_2O), Dutch wax print fabrics (21.613–21.659 mmH_2O), and cotton face coverings (15.857–15.905 mmH_2O). The high breathability observed in the present study may be explained by the generally low FE. Pressure differentiations (Δp) across the entire size range were also compared with the ASTM

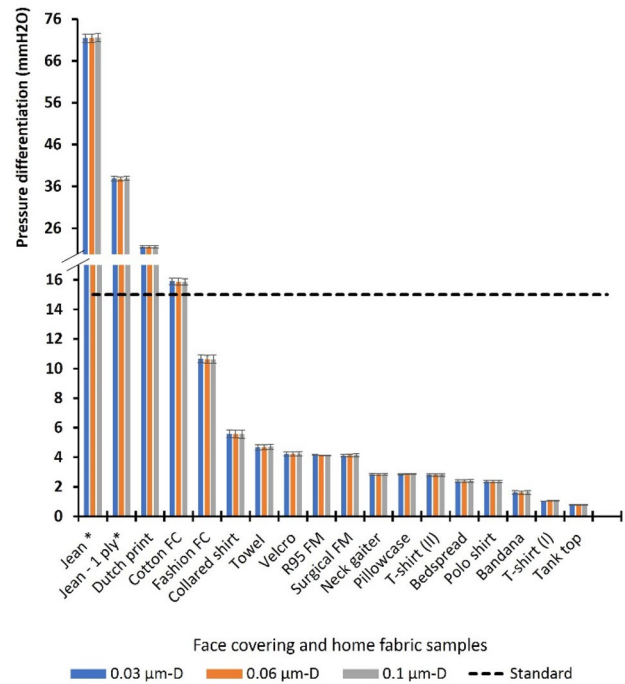


Fig. 3 Size-dependent breathability of barrier face coverings and home fabric samples. Horizontal dotted line represents the ASTM standard (F3502-21) threshold ($\leq 15 \text{ mmH}_2\text{O}$) for a low-performance face covering ($\leq 5 \text{ mmH}_2\text{O}$ for high performance)

Standard values of $> 15 \text{ mmH}_2\text{O}$ for lower performance and $< 5 \text{ mmH}_2\text{O}$ for higher performance barrier face coverings. The majority of the samples in the present study are breathable and have the high-performance Δp range suggested in the ASTM Standard (Fig. 3). Of all the total 16 different samples included in the study, only collared shirt (5.56–5.59 mmH_2O), Dutch wax print fabric (21.61–21.66 mmH_2O), fashion (10.63–10.66 mmH_2O), and cotton face coverings (15.86–15.91 mmH_2O) have Δp in the low-performance category.

The comparatively high Δp in Dutch wax prints may be due to the resins and dyes used in their production. The inter-fiber spaces of barrier face coverings are the pores that allow the passage of some particles including air. This is a key distinction in aerosol filtration models that establish what passes through or gets captured via direct impaction, diffusion, or interception. The waxes, paints or dye used on face covering samples can block many of the inter-fiber spaces thus increasing Δp , because transmission energy is inversely proportional to pore sizes (Aydin et al. 2020). Particle size does not seem to impact breathability (S. Table 3). The similarity observed in the correlation may be due to the small variation in breathability within each sample despite increasing particle size. The correlation between GSM and Δp is presented in Table 1.

Table 2 Fluorescence intensity (with standard deviation, SD) and the percentage flow of nanobeads estimated from fluorescence intensity of flow-through incident nanobead-containing droplets

Samples	I_{Sample}	SD	Flow (%)
2. Bandana	109.25	26.29	0.817
5. Neck gaiter	61.25	19.00	0.458
9. T-shirt (I)	108.75	41.47	0.813
11. Tank top	150.00	67.10	1.122
13. Bedspread	6.25	5.12	0.047

Nanobeads Flow Resistance and Overall Performance Evaluation

The experimental average percentage recoveries of nanobeads in 2.5, 5.0 and 20.0 μL challenge solution were 87.93%, 81.26% and 99.18%, respectively. The DF was 1.97 (± 0.056) and average fluorescence of I_{solution} was 13,371.30 (± 465.46). The percentage flow of latex beads was estimated from fluorescence intensity and presented in Table 2. Most of the tested samples resisted the flow of nanobead-containing droplets except bandana, neck gaiter masks, t-shirt I, tank top, and bedspread fabrics. The highest flow was recorded for tank top (1.12%) and the lowest was recorded for bedspread (0.05%). No specific flow pattern could be attributed to the fabric characteristics (thickness, density, weave type or material composition). As suggested by Aydin et al. (2020), the most likely explanation could be sample porosity. The backside illumination intensity method described by Aydin et al. (2020) can be used to evaluate the porosity of fabric samples used at alternative barrier face coverings. It should be noted that the flow-through fabrics were among the samples with the highest particle penetration ($100 - \text{FE}$) and highest breathability (lower Δp). Particle penetration ranges of bandana, neck gaiter, t-shirt I, tank top and bedspread were 74.98–95.84%, 70.55–90.38%, 66.16–91.92%, 77.45–93.48%, and 75.00–96.39%, respectively, while Δp were 1.45–1.46 mmH_2O , 2.84–2.86 mmH_2O , 1.04–1.06 mmH_2O , 0.78–0.80 mmH_2O , and 2.38–2.41 mmH_2O , respectively. These are among the lowest FE and Δp documented in the current study.

In the present study, the velocity of incident droplets ranged from 239.35 to 6252.29 cm/s measured within 1 cm from the nozzle of the bottle. The median velocity of tracked droplets ranged from 1007.58 to 1689.94 cm/s . The experimental set up mimicked a real-life sneezing scenario and how barrier face coverings can resist the flow of ejected droplets. The maximum droplet velocity of a typical sneeze was previously documented to range from 1200 to 1500 cm/s with varying droplet numbers (Bahl et al. 2020). The nanobead experiment was performed with respective number of layers of materials in already-made masks as sold and one

layer of home fabric samples. However, homemade fabrics are usually sewn using two layers. Therefore, the experiments were repeated only for the flow-through fabrics using two layers and no flow of nanobeads were recorded. It is important to note that it required two layers of neck gaiter and bandana samples to resist the flow of 0.1 μm nanobeads carried by droplets at 239.35 to 6252.29 cm/s . In general, the results of the present study indicated that the droplet blocking efficiency of most samples were high for single layers and no flow was observed for multiple-layered samples. The results are like the ones reported by Aydin et al. (2020) which indicated that the median droplet blocking efficiency of home fabrics was more than 70%, and at 2–3 layers, droplet blocking efficiency of home fabrics were comparable to that of medical face masks.

The statistically significant ($p < 0.05$) correlation between FE and breathability has been indicated by the results of the current study (Table 3) as supported by other studies (Kähler and Hain, 2020; Hao et al. 2020; Zhao et al. 2020; Bagheri et al. 2021). Since the relationships between FE and breathability were inverse, to determine the samples with an optimum performance, the overall performance (qF) of barrier face covering samples were estimated. This was achieved by combining both the FE and Δp using Eq. (2) that have been formulated to estimate the quality of filter samples by considering both parameters simultaneously. The qF of samples are provided in Table 4 and S. Table 4. Relative performance of samples to R95 masks is presented in Fig. 4a–d.

Dutch wax print (0.034), pillowcase (0.067), and bedspread (0.098) fabrics and fashion face covering (0.100) were samples with the lowest qF values. Velcro mask (3.362) with inner filter, surgical masks (3.494), t-shirt I (2.958) and tank top (2.418) fabrics were samples with the highest qF. The range of qF values for R95 mask was 12.334–13.374. In the current study, using the FE and Δp values suggested in the ASTM standard, qF for low-performance and

Table 3 Correlation between FE and breathability

D- μm	r_s	p value
0.030	0.527	0.035*
0.040	0.569	0.023*
0.050	0.574	0.022*
0.060	0.532	0.033*
0.080	0.529	0.034*
0.100	0.566	0.024*
0.150	0.527	0.035*
0.200	0.552	0.027*
0.250	0.586	0.019*
0.300	0.507	0.042*
0.350	0.505	0.043*
0.400	0.605	0.016*

*Significant at $p < 0.05$

Table 4 Density (GSM), FE and pressure differentiation (Δp) ranges of samples and their overall performance

Samples	GSM (g/m ²)	FE (%)	Δp (mmH ₂ O)	qF
1. Fashion face mask	298.33	13.27–38.14	10.63–10.66	0.100–0.338
2. Bandana	135.15	4.16–25.02	1.45–1.46	0.198–1.337
3. Velcro mask	304.49	79.44–84.95	4.23–4.25	2.798–3.362
4. Cotton face covering	430.11	28.22–75.76	15.86–15.91	0.157–0.668
5. Neck gaiter	202.53	9.62–29.45	2.84–2.86	0.266–0.918
6. Surgical mask	64.91	74.21–85.74	4.11–4.18	2.466–3.494
7. Jean/denim	407.74	65.23–93.88	71.43–71.60	0.111–0.293
8. Polo-style shirt	210.69	14.82–48.84	2.36–2.37	0.510–2.133
9. T-shirt I	116.66	8.09–33.84	1.04–1.06	0.602–2.958
10. Collared shirt	169.94	17.18–54.75	5.56–5.59	0.254–1.066
11. Tank top	189.15	6.52–22.56	0.78–0.80	0.638–2.418
12. Towel	430.89	28.20–70.17	4.67–4.70	0.530–1.940
13. Bedspread	118.07	3.11–25.00	2.38–2.41	0.098–0.900
14. Pillowcase	128.94	2.55–17.05	2.85–2.88	0.067–0.490
15. T-shirt II	161.69	6.61–27.10	2.79–2.80	0.183–0.848
16. Dutch wax print	94.57	9.26–28.79	21.61–21.66	0.034–0.118
17. R95 mask	544.90	99.89–99.94	4.12–4.16	12.334–13.374

high-performance barrier face coverings were estimated as 0.112 and 1.040, respectively. Twenty-five percent (25%) of the samples have at least one qF value below the value categorized as low at any of the particle sizes examined. Only 12.5% of the samples have a qF range that is higher than the qF value for high performance barrier face coverings across all particle sizes. Surgical and velcro masks ranked higher among common already-made masks. For particle size 0.03–0.10, t-shirt I, towel, tank top and Polo-style fabrics ranked higher among home fabrics for alternative face masks. Size-dependent performances were generally lower for particle size 0.15–0.40 and were similar in pattern to the sizes reported by Dhanraj et al. (2021). Many were below the qF value for a high-performance face covering (Table 4). Relative performance of samples with R95 mask is given in Fig. 4.

The high overall performance of R95, surgical and velcro masks are directly related to their higher FE and lower Δp . Similar performances at submicron and supermicron aerosol sizes have been reported (Liu and Zhao 2021). Size-dependent FE of samples were further highlighted when relative performances of samples were estimated against R95 masks. It should be noted that relative performances were lower at MPPS (Fig. 4c, d).

Conclusion

The question in the present study was whether commonly sold face coverings and those made from home fabrics used during the COVID-19 pandemic can both effectively block submicron particles and sustain sufficient breathability.

Because either can be the case for a particular sample, we evaluated overall performances using a mathematically formulated equation that simultaneously incorporates filtration efficiency and breathability. It was found that most samples have low size-dependent pressure differentiation (high breathability) and filtration efficiencies. Some samples have low droplet flow resistance but at double layers, all samples resisted the flow of nanoparticle-laden droplets. Most samples were at the lower spectrum provided in the ASTM standard. Only a few samples have overall performances ranges that were above the higher spectrum in the standard. It was observed that the efficiency and breathability varied considerably among fabrics.

The results indicated that increasing the number of fabric layers significantly increases the blocking efficiency of samples. A multi-layered fabric will increase the likelihood that pores of the separate layers are not aligned thereby decreasing porosity and penetration. Since increasing efficiency may compromise breathability, the selection of fabric materials with optimum or high performance is important for effective protection against respiratory infection through droplets and aerosols. Fabric characteristics (especially GSM, thickness) and finishing (waxing, dye, etc.) could be a significant factor in determining which fabric sample will be suitable to produce homemade face coverings. Samples containing significantly high degree of finishing should be avoided, if possible because of pores blockage which will increase filtration efficiency but reduce breathability and comfortability. The complexity in the design of and finishing on fabric samples made extrapolation to other fabric types difficult. It is recommended that each fabric sample get evaluated before use as a barrier face coverings or only tested samples should be

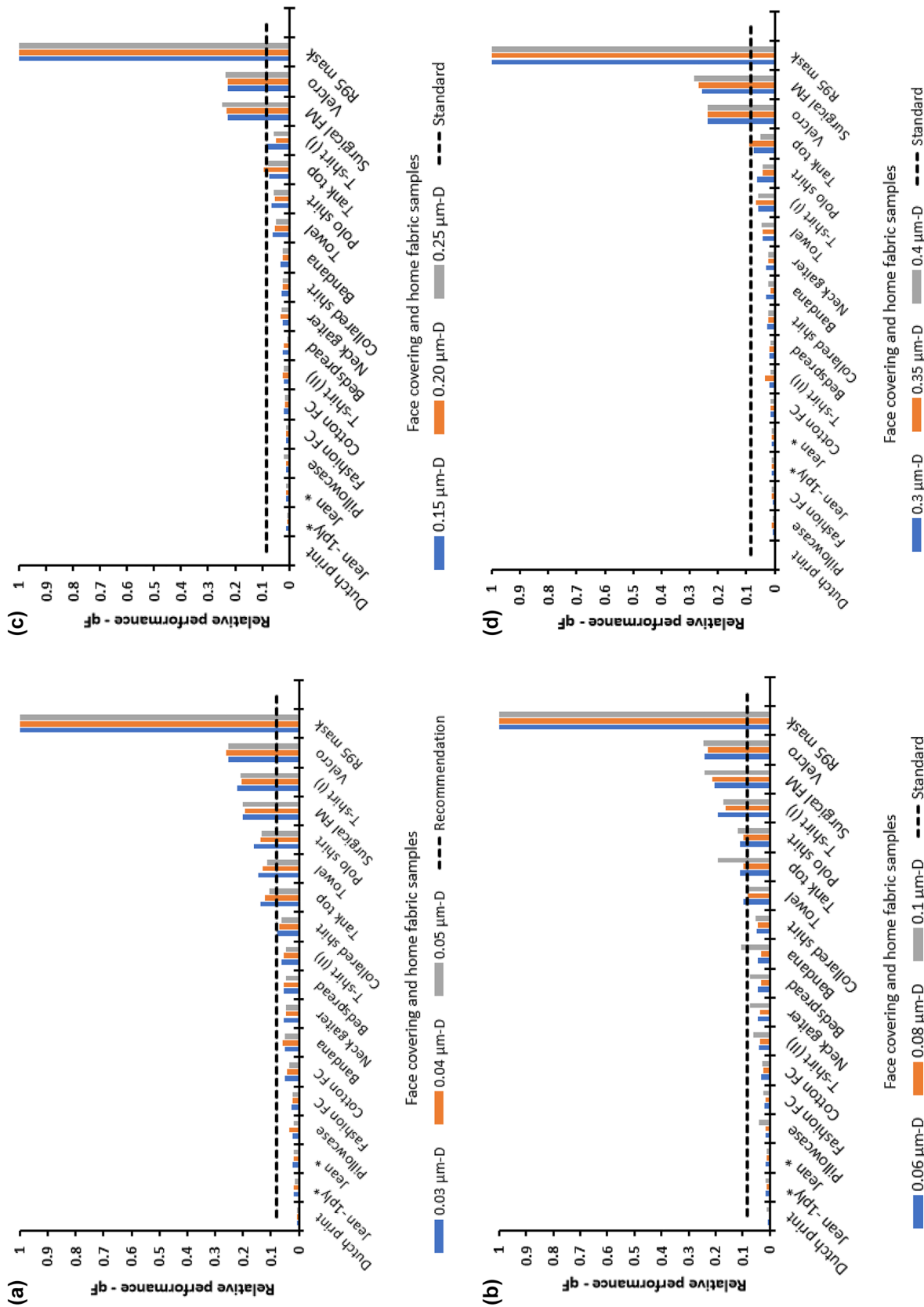


Fig. 4 Size-dependent relative performance of samples to R95 masks. The black dotted horizontal line represents qF for a high-performance (FE = 50%, $\Delta p = 5 \text{ mmH}_2\text{O}$) barrier face covering as recommended in the ASTM (F3502-21) standard

utilized. Future studies should focus on the standardization of outward leakages of barrier face coverings.

Supplementary Information The online version contains supplementary material available at <https://doi.org/10.1007/s41742-021-00390-6>.

Acknowledgements The authors would like to acknowledge Mirza Khyum for his contribution to fabric characterization and assistance with sample filtration. Seshadri Ramkumar gratefully acknowledges Cotton Incorporated for supporting the research on Health and Medical Protection Markets for Cotton.

Funding This work was supported by the Cotton Incorporated under Contract number 18–497.

Availability of Data and Materials Other supplementary information are presented in Supplementary Figures and tables.

Code Availability Not applicable.

Declarations

Conflict of Interest The authors declare that they have no conflict of interests.

References

- Abdelrahman Z, Li M, Wang X (2020) Comparative review of SARS-CoV-2, SARS-CoV, MERS-CoV, and influenza a respiratory viruses. *Front Immunol* 11:552909. <https://doi.org/10.3389/fimmu.2020.552909>
- American Society for Testing and Materials (2021) ASTM F3502 - 21: standard specification for barrier face coverings. Available at: <http://www.astm.org/cgi-bin/resolver.cgi?F3502-21>. Accessed on: 11/11/2021
- Aydin O, Emon B, Cheng S, Hong L, Chamorro LP, Saif MTA (2020) Performance of fabrics for home-made masks against the spread of COVID-19 through droplets: a quantitative mechanistic study. *Extreme Mech Lett* 40:100924. <https://doi.org/10.1016/j.eml.2020.100924>
- Ayodeji OJ, Ramkumar S (2021) Effectiveness of face coverings in mitigating the COVID-19 pandemic in the United States. *Int J Environ Res Public Health* 18:3666. <https://doi.org/10.3390/ijerph18073666>
- Bagheri MH, Khalaji I, Azizi A, Loibl RT, Basualdo N, Manzo S, Gorrepati ML, Mehendale S, Mohr C, Schiffres SN (2021) Filtration efficiency, breathability, and reusability of improvised materials for face masks. *Aerosol Sci Technol* 55:817–827. <https://doi.org/10.1080/02786826.2021.1898537>
- Bahl P, de Silva CM, Chughtai AA, MacIntyre CR, Doolan C (2020) An experimental framework to capture the flow dynamics of droplets expelled by a sneeze. *Exp Fluids* 61:176. <https://doi.org/10.1007/s00348-020-03008-3>
- Beck MJ, Hensher DA (2020) Insights into the impact of COVID-19 on household travel and activities in Australia—the early days under restrictions. *Transp Policy* 96:76–93. <https://doi.org/10.1016/j.tranpol.2020.07.001>
- Centers for Disease Control and Prevention (1996) NIOSH guide to the selection and use of particulate respirators. Available at: <https://www.cdc.gov/niosh/docs/96-101/default.html>. Accessed on: 11/11/2021
- Centers for Disease Control and Prevention (2020a) Coronavirus disease 2019 (COVID-19)—after you travel internationally. Available at: <https://www.cdc.gov/coronavirus/2019-ncov/travelers/after-travel-precautions.html>. Accessed on: 12/09/2020.
- Centers for Disease Control and Prevention (2020b) Strategies for optimizing the supply of facemasks. Available at: <https://www.cdc.gov/coronavirus/2019-ncov/hcp/ppe-strategy/face-masks.html>. Accessed on: 03/06/2021
- Cho H, Yoon C, Lee J, Lee S, Viner A, Johnson EW (2011) Comparison of pressure drop and filtration efficiency of particulate respirators using welding fumes and sodium chloride. *Ann Occup Hyg* 55:666–680. <https://doi.org/10.1093/annhyg/mer032>
- Dhanraj DIAD, Choudhary S, Jammalamadaka U, Ballard DH, Kumfer BM, Dang AJ, Williams BJ, Meacham KW, Axelbaum RL, Biswas P (2021) Size-dependent filtration efficiency of alternative facemask filter materials. *Materials* 14:1868. <https://doi.org/10.3390/ma14081868>
- Drewnick F, Pikmann J, Fachinger F, Moormann L, Sprang F, Borrmann S (2021) Aerosol filtration efficiency of household materials for homemade face masks: influence of material properties, particle size, particle electrical charge, face velocity, and leaks. *Aerosol Sci Technol* 55:63–79. <https://doi.org/10.1080/02786826.2020.1817846>
- Friedlander SK (2000) *Smoke, dust, and haze*. Oxford University Press, New York
- Gopalan HS, Misra A (2020) COVID-19 pandemic and challenges for socio-economic issues, healthcare and National Health Programs in India, diabetes and metabolic syndrome. *Clin Res Rev* 14:757–759. <https://doi.org/10.1016/j.dsx.2020.05.041>
- Hao W, Parasch A, Williams S, Li J, Ma H, Burken J, Wang Y (2020) Filtration performances of non-medical materials as candidates for manufacturing facemasks and respirators. *Int J Hyg Environ Health*. <https://doi.org/10.1016/j.ijheh.2020.113582>
- Hao W, Xu G, Wang Y (2021) Factors influencing the filtration performance of homemade face masks. *J Occup Environ Hyg* 18:128–138. <https://doi.org/10.1080/15459624.2020.1868482>
- Hinds W (1999) *Particle technology*. Wiley-Interscience, New York
- Johnson GR, Morawska L, Ristovski ZD, Hargreaves M, Mengersen K, Chao CYH, Wan MP, Li Y, Xie X, Katoshevski D, Corbett S (2011) Modality of human expired aerosol size distributions. *J Aerosol Sci* 42:839–851. <https://doi.org/10.1016/j.jaerosci.2011.07.009>
- Jones RM, Rempel D (2021) Standards for surgical respirators and masks: relevance for protecting healthcare workers and the public during pandemics. *Ann Work Exposures Health*. <https://doi.org/10.1093/annweh/wxab008>
- Joo T, Takeuchi M, Liu F, Rivera MP, Barr J, Blum ES, Parker E, Tipton JH, Varnedoe J, Dutta B, Lively RP, Lee Ng N (2021) Evaluation of particle filtration efficiency of commercially available materials for homemade face mask usage. *Aerosol Sci Technol* 55:930–942. <https://doi.org/10.1080/02786826.2021.1905149>
- Kähler CJ, Hain R (2020) Fundamental protective mechanisms of face masks against droplet infections. *J Aerosol Sci* 148:105617. <https://doi.org/10.1016/j.jaerosci.2020.105617>
- Konda A, Prakash A, Moss GA, Schmoltdt M, Grant GD, Guha S (2020) Aerosol filtration efficiency of common fabrics used in respiratory cloth masks. *ACS Nano* 14:6339–6347. <https://doi.org/10.1021/acsnano.0c03252>
- Kwong LH, Wilson R, Kumar S, Crider YS, Sanchez YR, Rempel D, Pillarisetti A (2021) Review of the breathability and filtration efficiency of common household materials for face masks. *ACS Nano* 15:5904–5924. <https://doi.org/10.1021/acsnano.0c10146>
- Li J, Leavey A, Wang Y, O'Neil C, Wallace MA, Burnham CAD, Boon AC, Babcock H, Biswas P (2018) Comparing the performance of 3 bioaerosol samplers for influenza virus. *J Aerosol Sci* 115:133–145

- Liu Y, Zhao B (2021) Size-dependent filtration efficiencies of face masks and respirators for removing SARS-CoV-2-laden aerosols. *Infect Control Hosp Epidemiol* 42:906–907. <https://doi.org/10.1017/ice.2020.366>
- Liu Y, Ning Z, Chen Y, Guo M, Liu Y, Gali NK, Sun L, Duan Y, Cai J, Westerdahl D, Liu X, Xu K, Ho K, Kan H, Fu Q, Lan K (2020) Aerodynamic analysis of SARS-CoV-2 in two Wuhan hospitals. *Nature* 582:557–560. <https://doi.org/10.1038/s41586-020-2271-3>
- Marroquin B, Vine V, Morgan R (2020) Mental health during the COVID-19 pandemic: effects of stay-at-home policies, social distancing behavior, and social resources. *Psychiatry Res* 293:113419. <https://doi.org/10.1016/j.psychres.2020.113419>
- Mofijur M, Rizwanul Fattah IM, Alam MA, Saiful Islam ABM, Ong HC, Rahman SMA, Najafi G, Ahmed SF, Uddin A, Mahlia TMI (2021) Impact of COVID-19 on the social, economic, environmental and energy domains: lessons learnt from a global pandemic. *Sustain Prod Consum* 26:343–359. <https://doi.org/10.1016/j.spc.2020.10.016>
- National Academies of Sciences, Engineering, and Medicine (2020) Rapid expert consultations on the COVID-19 Pandemic. Washington (DC): National Academies Press (US); 2020 Apr 30. Rapid Expert Consultation on the Possibility of Bioaerosol Spread of SARS-CoV-2 for the COVID-19 Pandemic (April 1, 2020) Available from: <https://www.ncbi.nlm.nih.gov/books/NBK556967/>
- Syed Q, Sopwith W, Regan M, Bellis MA (2003) Behind the mask. Journey through an epidemic: some observations of contrasting public health responses to SARS. *J Epidemiol Community Health* 57:855–856. <https://doi.org/10.1136/jech.57.11.855>
- Vincent JH (2007) Aerosol sample applications and field studies. In: Vincent JH (ed) *Aerosol sampling. Science, standards, instrumentation and applications*. Wiley, New York, pp 528–529
- WHO (2020a) Coronavirus disease (COVID-19): How is it transmitted? Available at: <https://www.who.int/news-room/q-a-detail/coronavirus-disease-covid-19-how-is-it-transmitted>. Accessed on: 09/12/2020.
- WHO (2020b) Transmission of SARS-CoV-2: implications for infection prevention precautions. Available at: <https://www.who.int/news-room/commentaries/detail/transmission-of-sars-cov-2-implications-for-infection-prevention-precautions>. Accessed on: 03/06/2021
- Zhang R, Li Y, Zhang AL, Wang Y, Molina MJ (2020) Identifying airborne transmission as the dominant route for the spread of COVID-19. *Proc Natl Acad Sci USA* 117:14857–14863. <https://doi.org/10.1073/pnas.2009637117>
- Zhao M, Liao L, Xiao W, Yu X, Wang H, Wang Q, Lin YL, Kilinc-Balci FS, Price A, Chu L, Chu MC, Chu S, Cui Y (2020) Household materials selection for homemade cloth face coverings and their filtration efficiency enhancement with triboelectric charging. *Nano Lett* 20:5544–5552. <https://doi.org/10.1021/acs.nanolett.0c02211>